*Korean J. Chem. Eng.*, **22**(2), 303-314 (2005)

# Simulation of Particle Deposition on Filter Fiber in an External Electric Field

**Hyun-Seol Park† and Young Ok Park**

Clean Air Technology Research Center, Korea Institute of Energy Research,
71-2, Jang-Dong, Yusung-Gu, Daejeon 305-343, Korea
(*Received 13 September 2004 • accepted 21 December 2004*)

**Abstract**–Particle deposition onto a filter fiber was numerically simulated when a uniform external electric field was applied. The effects of electric field strength, particle inertia, and electrical conductivity of particles on particle deposition characteristics such as particle loading patterns and collection efficiency were qualitatively investigated. As a result, the electrostatic forces between a newly introduced particle and the already captured particles on the fiber were found to have a great influence on the particle deposition patterns compared with the results where the electrostatic forces were neglected. Conductive particles and filter fibers lead to higher collection efficiency and more linear structure of particle deposits than those of dielectrics, and the particle inertia could also be more important to the collection efficiency of a fibrous filter when electric fields are present. The simulated particle deposits obtained from this work agreed well with the existing experimental results, in which the photographs of particle loaded fibers, within an external electric field, were reported.

Key words: Particle Deposition, Fibrous Filter, Electrostatic Force, External Electric Field, Simulation

## INTRODUCTION

Filtration performance of a fibrous filter is directly related to the internal structure of the filter [Park and Park, 2005; Park et al., 2001]. As dust particles are captured on the filter fibers, the filter structure is changed. Consequently, the filtration characteristics are varied with particle loading. During the initial stage of air filtration, particles are first captured on clean fibers, and are subsequently deposited onto the already deposited particles as well as on the fibers. The deposited particles form chain-like agglomerates on the fibers, which are called dendrites [Tien et al., 1977]. Generally, it is known that the particle loading on a fibrous filter leads to a substantial increase in the collection efficiency and pressure drop [Payatakes, 1976; Barot et al., 1980; Kanaoka and Hiragi, 1990; Hinds and Kadrichu, 1997; Sakano et al., 2000]. Therefore, the structure of particle deposits on a fiber has a big effect on the performance of air filters.

The morphology and growing process of particle dendrites on the fibers in a fibrous filter varies with the filtration conditions. In the presence of electrostatic forces, particles are deposited on the filter fibers in a quite different manner compared with the cases of no electrical forces. A few studies have been carried out on the particle loading of electrically enhanced air filters. Neilsen and Hill [1980] simulated deposition patterns of charged particles onto a fiber charged with the opposite polarity. Baumgartner and Löffler [1987] also conducted a three-dimensional simulation of the deposition of polydisperse particles on filter fibers. They showed the deposition patterns of particles having different size distributions on electrically charged or uncharged fibers. The effect of particle loading on the performance of electrically charged fibrous filters has been experimentally analyzed by Walsh and Stenhouse [1998]. They proved the charge of the collected particles had no effect on the filter degradation.

†To whom correspondence should be addressed.
E-mail: phs@kier.re.kr

Besides the electrical charging of filter fibers, the filtration performance of a fibrous filter can be improved by applying an external electric field across the filter. Many theoretical and experimental studies have been performed over recent decades, which have examined the effects of external electric fields on the collection efficiency of fibrous filters [Havlíček, 1961; Zebel, 1965; Kirsch, 1971; Iinoya and Makino, 1974; Nelson et al., 1978; Kao et al., 1987; Wu et al., 1999]. However, those are for clean air filters where no particles are collected.

For the studies on dust loading characteristics of air filters placed in electric fields, model filters have been used. Oak and Saville [1980] presented a number of pictures, taken with an electron microscope, of particle dendrites on an isolated fiber. In their experiments strong external electric fields were applied transversely to the fiber, and the particles were weakly charged. Under those conditions, linear dendrites, protruding in the direction of electric fields, were observed in the study. Wang et al. [1980] also conducted an experimental study on the accumulation of particles onto single fibers and the morphology of particle deposits in the presence of external electric fields, and showed the rates of particle deposition and dendrite growth for various external electric fields.

A theoretical analysis on the particle loading characteristics of air filters with applied electric fields can only be accomplished by using a numerical method, since the geometrical complexity of the particle deposited filter consequently results in complicated electric fields within the filter. Furthermore, the morphology of the dendrites on a fiber is continuously altered as particles are collected. For this reason, it is practically impossible to exactly analyze the particle deposition phenomena in real filters. Therefore, some approximations and assumptions should inevitably be used in theoretical studies on the particle loading of air filters enhanced by the application of an external electric field.

Auzerais et al. [1983] simulated the dendritic deposition of uncharged dielectric particles on an uncharged dielectric fiber in the

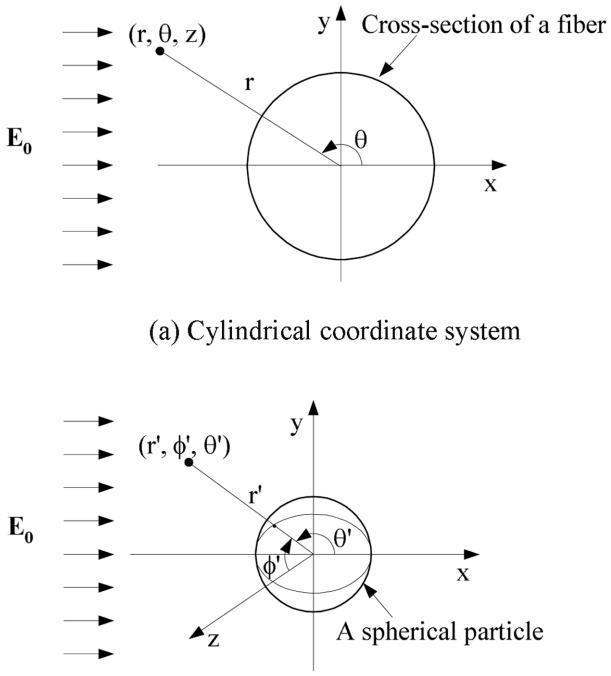


**Fig. 1. Coordinate systems of (r, $\theta$, z) and (r', $\phi'$, $\theta'$) used in this study.**

presence of an electric field. They assumed that the inertia of particles could be neglected for calculation simplicity, and a particle dendrite was approximated to be an ellipsoid of equal volume and height. They utilized the upper half of a fiber as a calculation domain for reducing the computation time. As a result, the dependency of the structure of deposits and deposition rate of particles on the electric field strength was shown.

In this study, the characteristics of particle deposition onto filter fibers in an electric field were thoroughly investigated to provide more information about the particle loading of air filters enhanced by the application of external electric fields. This was accomplished by examining the effects of particle inertia and the electrical properties of the particles and fibers on the particle deposition as well as the effects of electric field strength and electrostatic forces between the approaching particles and the previously collected particles. A Lagrangian approach was adopted to simulate the particle deposition. Conversely to the work of Auzerais et al. [1983], the electrical forces due to particle dendrites were calculated by the summation of the individual forces that correspond to each of the deposited particles, rather than approximating a dendrite to a single assembly. This method might lead to a more accurate prediction of the particle deposition. This work also provides three-dimensional views of the particle deposits on a fiber of finite length, which enables a direct understanding of the particle deposition phenomena.

## THEORY

### 1. Electric Fields and Electrostatic Forces

When an external electric field is applied across a fibrous filter, dust particles passing through the filter experience several types of electrostatic forces. Assuming that all the filter fibers have no electrical charges, the electrostatic forces acting on a particle flowing through the filter are the Coulombic force due to the particle charge and the dielectrophoretic force due to the polarization of the particle. The Coulombic force is simply calculated by multiplication of the particle charge with the electric field strength at a given position, whereas the dielectrophoretic force is dependent on the polarizability of the particle and the non-uniformity of the electric fields. Therefore, the electric fields and forces concerned have to initially be found. The electrostatic forces in fibrous filters and their effect on filtration performance have been comprehensively reviewed by Shapiro et al. [1983], Brown [1993], and Wang [2001].

For a clean filter fiber, transversely placed in a uniform electric field of strength $E_0$, the electric field around the fiber is given with cylindrical coordinates of (r, $\theta$, z) as follows. The coordinate system is shown in Fig. 1(a).

$$E_r = \left(\frac{\varepsilon_f - 1}{\varepsilon_f + 1}\frac{r_f^2}{r^2} + 1\right) E_0 \cos\theta, \tag{1a}$$

$$E_\theta = \left(\frac{\varepsilon_f - 1}{\varepsilon_f + 1}\frac{r_f^2}{r^2} - 1\right) E_0 \sin\theta, \tag{1b}$$

$$E_z = 0, \tag{1c}$$

where $E_0$, $E_r$, $E_\theta$, and $E_z$ denote the given external electric field strength, the radial, tangential, and z directional components of the electric field, respectively. $\varepsilon_f$ is the dielectric constant, and $r_f$ the fiber radius. Since the electric field around the fiber is axisymmetric, the z directional component, $E_z$, is zero.

As particles are gradually captured on a fiber, the electric field around the fiber changes due to deposited particles. For a more accurate simulation, these changes must be taken into consideration. In the present study it is assumed that the electric field around a fiber with deposited particles can be obtained by superposition of the electric fields around each of the captured particles and the electric field around the clean fiber. This superposition method was used in the study of Auzerais et al. [1983], who proved the validity of these approximations.

Using the three dimensional Cartesian coordinates x, y, and z, and the spherical coordinates r', $\phi'$, and $\theta'$, as shown in Fig. 1(b), the electric field around a spherical particle placed in a homogenous external electric field, $E_0$, is

$$E_{r'} = \left(\frac{\varepsilon_p - 1}{\varepsilon_p + 2}\frac{2r_p^3}{r'^3} + 1\right) E_0 \cos\theta', \tag{2a}$$

$$E_{\phi'} = 0, \tag{2b}$$

$$E_{\theta'} = \left(\frac{\varepsilon_p - 1}{\varepsilon_p + 2}\frac{r_p^3}{r'^3} - 1\right) E_0 \sin\theta', \tag{2c}$$

where $E_{r'}$, $E_{\phi'}$, and $E_{\theta'}$ are the radial, longitudinal, and latitudinal components of the electric field, respectively. $\varepsilon_p$ is the dielectric constant and $r_p$ the particle radius. Here, the longitudinal component, $E_{\phi'}$ is zero because of the axisymmetric property of the electric field in the direction of the x-axis. Therefore, the resultant electric field around those particles can be simply calculated as

$$E_{r',total} = \sum_{k=1}^{N} E_{r'_k} = E_0 \sum_{k=1}^{N} \left(\frac{\varepsilon_p - 1}{\varepsilon_p + 2}\frac{2r_p^3}{r_k'^3} + 1\right) \cos\theta'_k, \tag{3a}$$

$$E_{\phi',total} = \sum_{k=1}^{N} E_{\phi'_k} = 0, \tag{3b}$$

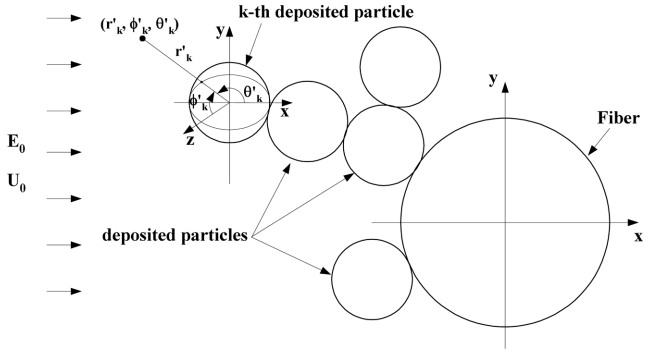


**Fig. 2. A spherical coordinate system of ($r'_k$, $\phi'_k$, $\theta'_k$), whose origin is located at the center of the k-th deposited particle.**

$$E_{\theta',total}=\sum_{k=1}^{N}E_{\theta'_k}=E_0\sum_{k=1}^{N}\left(\frac{\varepsilon_p-1}{\varepsilon_p+2}\frac{r_p^3}{r_k'^3}-1\right)\sin\theta'_k, \tag{3c}$$

where N is the total number of collected particles, and $r'_k$, $\phi'_k$, and $\theta'_k$ represent the spherical coordinates whose origin is located at the center of the k-th deposited particle as illustrated in Fig. 2.

From Eqs. (1a)-(1c), (2a)-(2c), and (3a)-(3c), the electric field around a particle loaded fiber in an external electric field in the coordinate system (x, y, z) is obtained as follows.

$$E_{x,total}=E_r\cos\theta-E_\theta\sin\theta+\sum_{k=1}^{N}(E_{r'_k}\cos\theta'_k-E_{\theta'_k}\sin\theta'_k) \tag{4a}$$

$$E_{y,total}=E_r\sin\theta+E_\theta\cos\theta+\sum_{k=1}^{N}(E_{r'_k}\sin\theta'_k-E_{\theta'_k}\cos\theta'_k)\sin\phi_k \tag{4b}$$

$$E_{z,total}=\sum_{k=1}^{N}(E_{r'_k}\sin\theta'_k-E_{\theta'_k}\cos\theta'_k)\cos\phi_k \tag{4c}$$

One of the most important purposes of the present study is to investigate the effect of the electrostatic interactions between an oncoming particle and the already loaded particles on particle deposition. Therefore, the electrostatic forces due to the deposited particles should be contained in the governing equation.

When a spherical particle, with some electric charge, flows past a dust loaded filter fiber within an external electric field, it experiences the electrostatic forces as expressed below Eq. (5), in a vector form. In this study, the electrostatic system of units (e.s.u.) was used to describe the electrostatic forces.

$$\vec{F}_E=q_p\left(\vec{E}+\sum_{k=1}^{N}\vec{E}_k\right)+\frac{r_p^3}{2}\left(\frac{\varepsilon_p-1}{\varepsilon_p+2}\right)\nabla\left|\vec{E}+\sum_{k=1}^{N}\vec{E}_k\right|^2, \tag{5}$$

where $q_p$ is the particle charge, $r_p$ the particle radius, $\varepsilon_p$ the dielectric constant of particle, N the total number of deposited particles, $\vec{E}$ the electric field around a fiber, $\vec{E}_k$ the electric field around the k-th deposited particle, and $\vec{F}_E$ the electrostatic force.

In Eq. (5) the first term of the right hand side is the Coulombic force due to the particle charge, and the second is the dielectrophoretic force due to the particle polarization and nonhomogeneity of the electric fields. According to Eq. (5), the dielectrophoretic force must be calculated only after obtaining the square of the magnitude of a resultant electric field vector, which is the summation of the electric field around a clean fiber and the fields around each of particles captured on the fiber. In practice, however, it is impossible to follow the procedure in mathematical modeling; thus an approximated method is adopted in this study. The approximation assumes that the dielectrophoretic force calculated according to the above procedure is equal to the sum of polarization forces between the oncoming particle and each of the captured particles, and the polarization force between the particle and the fiber. The validity of the approximated calculation was proved by Auzerais et al. [1983]. Subsequently rearranging Eq. (5), the following equation is obtained.

$$\vec{F}_E=q_p\left(\vec{E}+\sum_{k=1}^{N}\vec{E}_k\right)+\frac{r_p^3}{2}\left(\frac{\varepsilon_p-1}{\varepsilon_p+2}\right)\left(\nabla|\vec{E}|^2+\sum_{k=1}^{N}\nabla|\vec{E}_k|^2\right). \tag{6}$$

Besides the forces mentioned above, the image force, due to the particle charge, and the dielectrophoretic force, due to the polarization of a fiber by the electric field around the oncoming particle, are neglected owing to their relatively small magnitudes.

## 2. Governing Equation of Particle Motion

The first step in the simulation of particle deposition patterns on a filter fiber is the calculation of the particle trajectories. A particle trace can be obtained by solving an equation of motion of the particle concerned. Assuming there are no Brownian diffusion effects, the equation of motion of a particle moving through a fibrous filter placed in a uniform external electric field, is written as

$$m\frac{d\vec{v}}{dt}=\vec{F}_D+\vec{F}_E+\vec{F}_G, \tag{7}$$

where m is the mass of the particle, $\vec{v}$ the velocity of the particle, $\vec{F}_D$ the drag force generated by the difference in the velocities of fluid and the particle, $\vec{F}_E$ the electrostatic force exerted on the particle, and $\vec{F}_G$ the gravitational force. $\vec{F}_D$ can be expressed in several different forms, according to the value of Reynolds number (Re). Under the filtration condition of this study Re is less than 1; thus the drag force, $\vec{F}_D$, is

$$\vec{F}_D=\frac{3\pi\mu d_p}{C_c}(\vec{u}-\vec{v}), \tag{8}$$

where $d_p$ is the particle diameter, $\mu$ the kinetic viscosity of air, $\vec{u}$ and $\vec{v}$ are the velocities of fluid and the particle, respectively, and $C_c$ is the coefficient that corrects the slip effect between a particle and air molecules. Here, $C_c$ by Jennings [1988] was used. As a flow model in a fibrous filter, the flow field suggested by Henry and Ariman [1981] was employed for this study. The flow model, where the possibility of slip flow at the fiber surface is taken into account, is modified from the Kuwabara flow field [Kuwabara, 1959]. The radial and tangential components of the flow field are described by

$$u_r=\frac{2U_0}{J}\left\{A\left(\frac{r_f}{r}\right)^2+B+C\ln\left(\frac{r}{r_f}\right)+D\left(\frac{r}{r_f}\right)^2\right\}\cos\theta, \tag{9a}$$

$$u_\theta=\frac{2U_0}{J}\left\{A\left(\frac{r_f}{r}\right)^2-B-C-C\ln\left(\frac{r}{r_f}\right)-3D\left(\frac{r}{r_f}\right)^2\right\}\sin\theta, \tag{9b}$$

where

$$J=3+2\ln c-4c+c^2+Kn(2+4\ln c-2c^2), \tag{10a}$$

$$A=\frac{c}{2}-1-cKn,\ B=1-c,\ C=-4\left(\frac{1}{2}+Kn\right),\ D=\left(\frac{1}{2}+Kn\right)c, \tag{10b}$$

$$c=\left(\frac{r_f}{b}\right)^2,\ Kn=\frac{\lambda}{r_f}. \tag{10c}$$

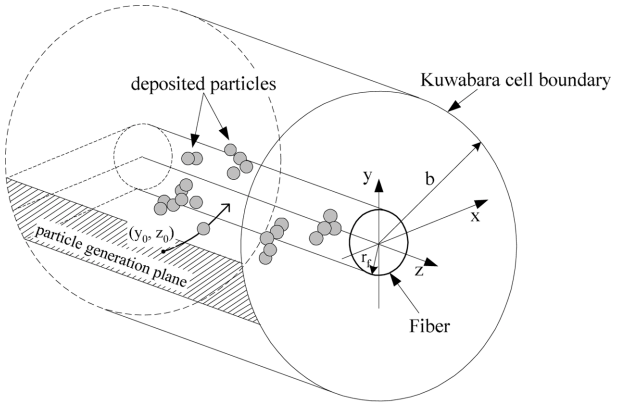


**Fig. 3. Single fiber model adopted in this study.**

In Eqs. (10a)-(10c), c denotes the packing density of a filter, b the radius of Kuwabara cell depicted in Fig. 3, Kn the dimensionless parameter called Knudsen number, and $\lambda$ the mean free path of air molecules.

The gravitational force, $\vec{F}_G$, can be expressed as

$$\vec{F}_G = \frac{\pi d_p^3}{6}(\rho_p - \rho_{air})\cdot\vec{g}, \tag{11}$$

where $\rho_p$ is the particle density, $\rho_{air}$ the fluid density, and $\vec{g}$ the gravitational acceleration. Substituting Eqs. (6), (8), and (11) into Eq. (7), the following equation is obtained.

$$m\frac{d\vec{v}}{dt} = \frac{3\pi\mu d_p}{C_c}(\vec{u}-\vec{v}) + \frac{\pi d_p^3}{6}(\rho_p-\rho_{air})\cdot\vec{g} + q_p\left(\vec{E}+\sum_{k=1}^{N}\vec{E}_k\right) + \frac{r_p^3}{2}\left(\frac{\varepsilon_p-1}{\varepsilon_p+2}\right)\left(\nabla|\vec{E}|^2+\sum_{k=1}^{N}\nabla|\vec{E}_k|^2\right). \tag{12}$$

The above equation cannot be solved analytically; thus the solution can be obtained only by numerical methods. For the numerical calculation, Eq. (12) is divided into the three components of a Cartesian coordinate system of (x, y, z), and each component equation is transformed into a dimensionless form for easier manipulation. The final form of the governing equation is

$$\frac{dv_x^*}{dt^*} = (u_x^*-v_x^*)/Stk + (N_{REP}/Stk)\sum_{k=1}^{N}\cos\theta'_k + (N_C/Stk)\left[(F^*_{C,r}\cos\theta - F^*_{C,\theta}\sin\theta) + \sum_{k=1}^{N}(F^*_{C,r'_k}\cos\theta'_k - F^*_{C,\theta'_k}\sin\theta'_k)\right] + (N_{P,I}/Stk)(F^*_{P,r}\cos\theta - F^*_{P,\theta}\sin\theta) + (N_{P,II}/Stk)\sum_{k=1}^{N}[F^*_{P,r'_k}\cos\theta'_k - F^*_{P,\theta'_k}\sin\theta'_k] \tag{13a}$$

$$\frac{dv_y^*}{dt^*} = (u_y^*-v_y^*)/Stk + (N_{REP}/Stk)\sum_{k=1}^{N}\sin\theta'_k\sin\phi'_k + N_G/Stk + (N_C/Stk)\left[(F^*_{C,r}\sin\theta + F^*_{C,\theta}\cos\theta) + \sum_{k=1}^{N}(F^*_{C,r'_k}\sin\theta'_k + F^*_{C,\theta'_k}\cos\theta'_k)\sin\phi'_k\right] + (N_{P,I}/Stk)[(F^*_{P,r}\sin\theta - F^*_{P,\theta}\cos\theta) + (N_{P,II}/Stk)\sum_{k=1}^{N}[F^*_{P,r'_k}\sin\theta'_k - F^*_{P,\theta'_k}\cos\theta'_k]\sin\phi'_k \tag{13b}$$

$$\frac{dv_z^*}{dt^*} = (u_z^*-v_z^*)/Stk + (N_{REP}/Stk)\sum_{k=1}^{N}\sin\theta'_k\cos\theta'_k + (N_C/Stk) + \sum_{k=1}^{N}[F^*_{C,r'_k}\sin\theta'_k + F^*_{C,\theta'_k}\cos\theta'_k]\cos\theta'_k, + (N_{P,II}/Stk) + \sum_{k=1}^{N}[F^*_{P,r'_k}\sin\phi'_k - F^*_{P,\theta'_k}\cos\theta'_k]\cos\theta'_k \tag{13c}$$

where

$$x^*=x/r_f,\quad y^*=y/r_f,\quad z^*=z/r_f,\quad t^*=U_0t/r_f, \tag{14a}$$

$$v_x^*=v_x/U_0,\quad v_y^*=v_y/U_0,\quad v_z^*=v_z/U_0, \tag{14b}$$

$$u_x^*=u_x/U_0,\quad u_y^*=u_y/U_0,\quad u_z^*=u_z/U_0, \tag{14c}$$

where $U_0$ is the undisturbed flow velocity normal to the axis of fiber, $v_x$, $v_y$, and, $v_z$ and $u_x$, $u_y$, and, $u_z$ are the x, y, and z components of particle and flow velocity, respectively.

In Eq. (13), Stk represents the Stokes number, $N_C$ is a dimensionless parameter describing the effect of the Coulombic force, and $N_{P,I}$ and $N_{P,II}$ denote dimensionless parameters associated with the polarization forces due to electric fields around the fiber and the captured particles, respectively. $N_{REP}$ is a dimensionless repellent force parameter, and $N_G$ the gravitational force parameter. All these dimensionless numbers represent the relative magnitudes of the electrostatic forces, inertial, or gravitational force to drag force acting on an approaching particle flowing past a particle-deposited filter fiber. Those parameters are expressed as

$$Stk = \frac{\rho_p d_p^2 U_0 C_c}{18\mu r_f}, \qquad N_C = \frac{q_p E_0}{3\pi\mu U_0 d_p/C_c}, \tag{15a}$$

$$N_{P,I} = \frac{2\alpha\beta r_p^2 E_0^2 (r_p/r_f)}{3\pi\mu U_0 d_p/C_c}, \qquad N_{P,II} = \frac{\beta^2 r_p^2 E_0^2 (r_p/r_f)^4}{3\pi\mu U_0 d_p/C_c}, \tag{15b}$$

$$N_{REP} = \frac{q_p^2/r_f^2}{3\pi\mu U_0 d_p/C_c}, \qquad N_G = \frac{d_p^2(\rho_p-\rho_{air})g}{18\mu U_0/C_c}, \tag{15c}$$

where

$$\alpha = \frac{\varepsilon_f - 1}{\varepsilon_f + 1}, \qquad \beta = \frac{\varepsilon_p - 1}{\varepsilon_p + 2}. \tag{16}$$

In the dimensionless governing equation $F^*_{C,r}$, $F^*_{C,\theta}$, $F^*_{C,r'_k}$ and $F^*_{C,\theta'_k}$ are the dimensionless Coulombic forces exerted on a charged particle along the electric field lines around the fiber, and around the k-th deposited particle, respectively.

$$F^*_{C,r} = \left(\alpha\left(\frac{1}{r^*}\right)^2 + 1\right)\cos\theta, \tag{17a}$$

$$F^*_{C,\theta} = \left(\alpha\left(\frac{1}{r^*}\right)^2 - 1\right)\sin\theta, \tag{17b}$$

$$F^*_{C,r'_k} = \left(2\beta\left(\frac{r_p}{r_f}\right)^3\left(\frac{1}{r'^*_k}\right)^3 + 1\right)\cos\theta'_k, \tag{17c}$$

$$F^*_{C,\theta'_k} = \left(\beta\left(\frac{r_p}{r_f}\right)^3\left(\frac{1}{r'^*_k}\right)^3 - 1\right)\sin\theta'_k, \tag{17d}$$

where $r^*$ and $r'^*_k$ are the dimensionless radial coordinates expressed as $r^*=r/r_f$ and $r'^*_k=r'_k/r_f$, respectively.

$F^*_{P,r}$, $F^*_{P,\theta}$, $F^*_{P,r_k}$ and $F^*_{P,\theta_k}$ are the dimensionless dielectrophoretic forces attributed to the polarization of the approaching particle and the nonuniformity of electric fields in the vicinity of the fiber and the k-th deposited particle.

$$F^*_{P,r} = -\left(\frac{1}{r^*}\right)^3\left[\beta\left(\frac{1}{r^*}\right)^2 + \cos 2\theta\right], \tag{18a}$$

$$F^*_{P,\theta} = -\left(\frac{1}{r^*}\right)^3 \sin 2\theta, \tag{18b}$$

$$F^*_{P,r'_k} = -\left(\frac{1}{r^*_k}\right)^4\left\{\left[4\beta\left(\frac{r_p}{r_f}\right)^3\left(\frac{1}{r^*_k}\right)^3 + 2\right]\cos^2\theta'_k - \left[\beta\left(\frac{r_p}{r_f}\right)^3\left(\frac{1}{r^*_k}\right)^3 + 1\right]\sin^2\theta'_k\right\}, \tag{18c}$$

$$F^*_{P,\theta'_k} = -\left(\frac{1}{r^*_k}\right)^4\left[\frac{5}{6}\beta\left(\frac{r_p}{r_f}\right)^3\left(\frac{1}{r^*_k}\right)^3 + 1\right]\sin 2\theta'_k. \tag{18d}$$

## NUMERICAL SIMULATION

The filter model adopted in this study is shown in Fig. 3, where b is the radius of the Kuwabara cell and $r_f$ is the fiber radius. The first step in a simulation is to determine how to generate the particles. For similarity to a real filtration, monodisperse particles are generated using a random process. RNUN, a random number generator in IMSL routines, was used in this work. It generates a sequence of uniform pairs ($y_0$, $z_0$) of pseudorandom numbers from a uniform distribution between 0 and 1. $y_0$ and $z_0$ are the initial positions of a particle in the y and z directions. Then, $x_0$, the initial position in the x direction, is calculated by $x_0 = -\sqrt{(b/r_f)^2 - y_0^2}$. As seen in Fig. 3, the dimensionless scales of the particle generation plane are 2 and 10 in the y and z direction, respectively. The sequences of the random numbers ($y_0$, $z_0$) were same for each simulation in order to make consistent comparison of the simulation results.

In this study, it is assumed that the flow velocity on the Kuwabara cell boundary is ($U_0$, 0, 0) in a coordinate system of (x, y, z) depicted in Fig. 3, where $U_0$ is the undisturbed flow velocity. Therefore, a particle starting from the particle generation plane has the initial velocity of ($U_0$, 0, 0). In addition, the direction of the external electric field of ($E_0$, 0, 0) is also parallel to x-axis and transverse to the fiber axis.

If the initial conditions are given, the particle trajectory can be numerically computed, using the 4-th order Runge-Kutta Method, from Eqs. (13a)-(13c). In this simulation, it was assumed that a particle is captured only when the approaching particle is deposited on the fiber surface or already deposited particles. That is, when the distance between the center of the fiber and the approaching particle is less than the sum of the particle radius and the fiber radius, and when the distance between the approaching particle and the captured particles is less than the particle diameter, the deposition occurs. The calculation is terminated when either the approaching particles reach the Kuwabara cell boundary, or the extruded particle dendrites touch the cell boundary. The effects of rebound and re-entrainment of the deposited particles were not considered.

As for the electrical charge of the particles, it was assumed that the particles were in a Boltzmann charge equilibrium state, which is generally accepted as the charge distribution of atmospheric aerosol particles. The fraction of particles having n units of charge of one sign, denoted $f(n)$, is expressed as follows [Keefe et al., 1959].

$$f(n) = \sqrt{\frac{e^2}{d_p kT\pi}}\exp\left(\frac{-n^2e^2}{d_p kT}\right), \tag{19}$$

where e is the elementary charge, n the number of elementary charge, $d_p$ the particle diameter, k the Boltzmann constant, and T the absolute temperature.

**Table 1. Values of parameters used in the present study**

| Parameters | Values |
|---|---|
| Particle diameter, $d_p$ | 2 μm |
| Fiber diameter, $d_f$ | 10 μm |
| Undisturbed flow velocity, $U_0$ | 5, 30 cm/s |
| Packing density of filter, c | 0.05 |
| Particle density, $\rho_p$ | 1 g/cm$^3$ |
| External electric field strength, $E_0$ | 5, 10, 15, 20 kV/cm |
| Particle charge, $q_p$ | Boltzmann equilibrium |
| Dielectric constant of particle, $\varepsilon_p$ | 4, ∞ |
| Dielectric constant of fiber, $\varepsilon_f$ | 4, ∞ |
| Viscosity of air, $\mu$ | $1.82\times10^{-4}$ P |
| Mean free path of air molecules, $\lambda$ | 0.065 μm |

The simulation conditions used in this study are summarized in Table 1. The particle size was 2 μm in diameter, so the Brownian diffusion was neglected. The sizes of the particle and fiber, the packing density, the particle density, and the particle charge were fixed throughout, as shown in Table 1, mentioned otherwise. For the conductive particles and fibers, the dielectric constant was assumed as infinity, while the value was set to 4 for the dielectrics.

## RESULTS AND DISCUSSION

The morphology of the particle accumulated on a filter fiber depends on the particle collection mechanisms of air filtration [Kanaoka et al., 1986]. Assuming no electrostatic interactions, interception, inertial impact, and Brownian diffusion are the major mechanisms. In this study, however, the electrostatic forces play a very important role in the particle deposition, whereas the Brownian diffusion effect is small enough to be negligible, as noted before.

In the present study, the particle loading characteristics of fibrous air filters were investigated by using a Lagrangian simulation method, with a uniform external electric field applied across the filter. Specifically, the effect of the electric field strength, the conductivity of particles and fibers, and particle inertia on the morphology of particle deposits and the collection efficiency were analyzed on the basis of the simulation results. The Lagrangian simulation provides more exact information on the effect of the filtration parameters on the filter performance such as collection efficiency, and particle loading, etc. Therefore, it is expected that the morphological characteristics of the particle deposits on filter fibers in an electric field can be largely understood from this work.

### 1. Effect of Electric Field Strength

Fig. 4 shows the particle deposition patterns on a cylindrical filter fiber when a uniform external electric field is applied across the fiber. The particle density was set to 1 g/cm$^3$, and the particles and fiber were regarded as conductors. The flow direction was normal to fiber and from left to right in Fig. 4, and parallel to that of the electric field applied. When the electric field is absent, particles are captured only by interception and inertial impact, and the deposited particles are irregularly agglomerated. For the case when an electric field is externally applied, the particles are deposited in a

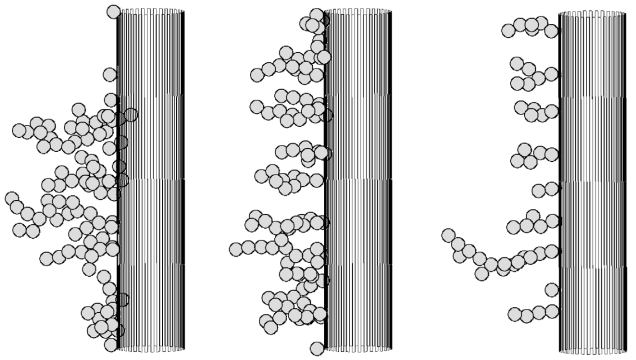

(a) $E_0$ = 0 kV/cm (b) $E_0$ = 10 kV/cm (c) $E_0$ = 20 kV/cm

**Fig. 4. Particle deposits on a fiber at the externally applied uniform electric field strength, $E_0$, of 0 kV/cm, 10 kV/cm, and 20 kV/cm, and the undisturbed flow velocity, $U_0$, of 5 cm/s.**

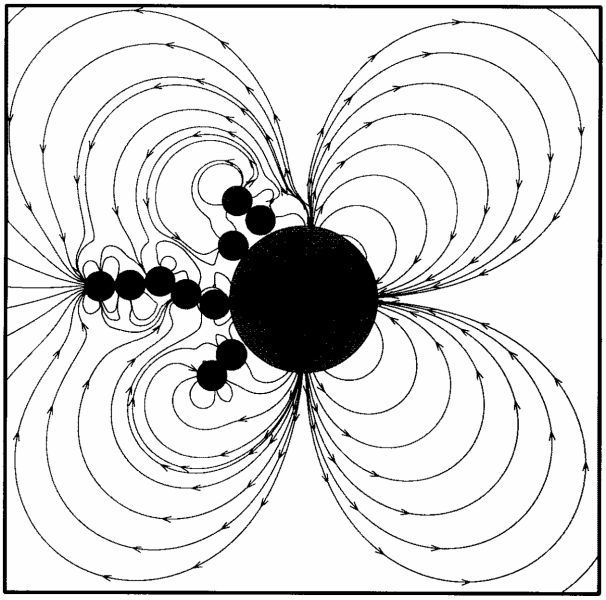

**Fig. 5. Dielectrophoretic force lines in the vicinity of a particle-deposited fiber within a uniform electric field.**

somewhat arranged pattern. As can be seen in Fig. 4(b)-4(c), the dendrites, which is the chain-like deposit of particles, become linear with increasing electric field strength. The linear structure is due to electrostatic forces. Fig. 5 shows the dielectrophoretic force lines in the vicinity of a particle-loaded fiber within a uniform electric field. The direction of the electric field was from left to right, and the deposited particles were arbitrarily positioned. The plotted force lines are those of the electrostatic force calculated by the approximated method mentioned before. The external electric field polarizes the fiber and the deposited particles, and the electric forces due to the polarization converge on the front and rear sides of the fiber and the deposited particles. At the tip of the dendrites, especially, the attractive force lines are focused. This is why the approaching particles are deposited at the end of each dendrite. In addition the dielectrophoretic force is proportional to the second power of the electric field strength, $E_0$, as expressed in Eq. (15b), thus the particle

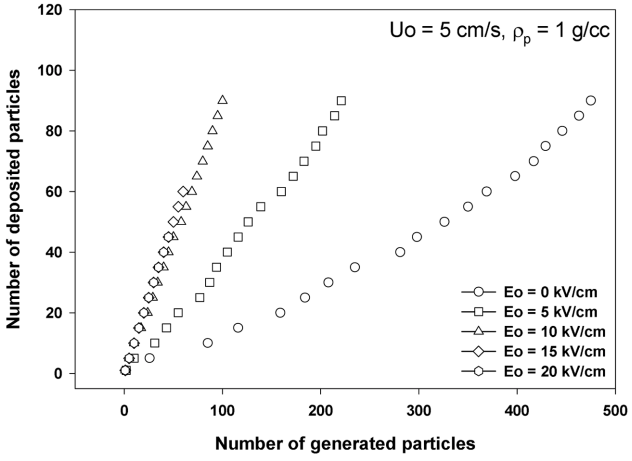


(a) $U_0$ = 5 cm/s

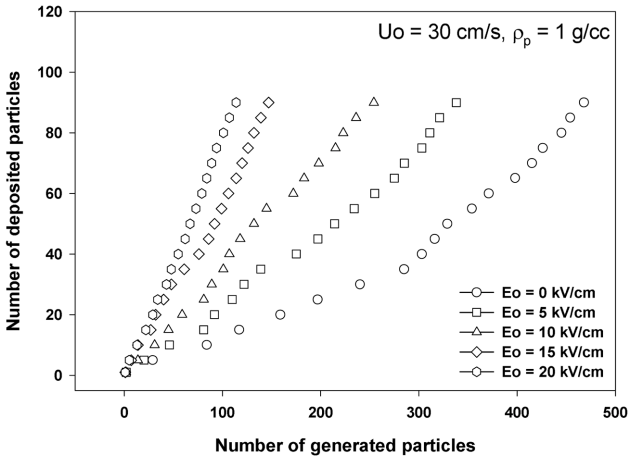


(b) $U_0$ = 30 cm/s

**Fig. 6. Deposition rate of particles on a fiber for various external electric fields at flow velocities of 5 cm/s and 30 cm/s.**

deposits become more linear as $E_0$ increases.

Fig. 6 is a graphical representation of the number of deposited particles with the x-axis denoting the number of generated particles at various external electric field strengths ranging from 0 to 20 kV/cm. The other simulation conditions were the same as in Fig. 4. In Fig. 6, the deposition rate, which can be defined by the gradient of the imaginary line for each symbol, actually represents the deposition ratio, $N/N_0$, where N is the number of deposited particles and $N_0$ is the total number of generated particles. From Fig. 6, it can be seen that the deposition rate became higher with increasing electric field strength, as expected. At $U_0$=5 cm/s, the deposition rates, with 10, 15, and 20 kV/cm, were almost same. On the other hand, at $U_0$= 30 cm/s, certain differences existed between them. When the flow velocity was small, the effect of electrostatic forces on particle deposition became larger than in the case of high flow velocity. Therefore, at $U_0$=5 cm/s, the collection efficiency was much higher than at $U_0$=30 cm/s.

**2. Effect of Electrostatic Forces due to Deposited Particles**

Fig. 7 shows the effect of the electrostatic forces between an approaching particle and the already deposited particles on the morphology of the particle deposits. With no electrostatic forces, an on-

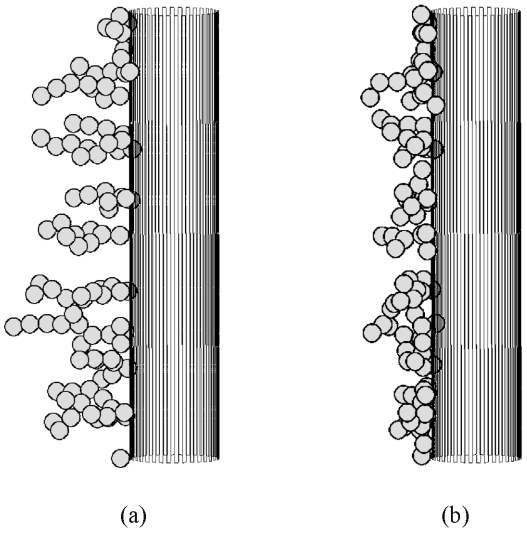


**Fig. 7. Particle deposition patterns simulated with and without the electrostatic forces between an approaching particle and the already deposited particles on a fiber at $E_0$=10 kV/cm and $U_0$=5 cm/s: (a) With electrostatic forces due to deposited particles, (b) Without electrostatic forces due to deposited particles.**

coming particle is captured due to only the dielectrophoretic force between the particles and the fiber. Therefore, the particles are packed more densely on the fiber surface, whereas the deposits have more porous and linear structures in the case where the electrostatic forces due to the collected particles are considered. The numbers of deposited particles plotted in Fig. 7 are 100 for both cases. The other simulation conditions are the same as used in Fig. 4.

Using the data of Fig. 7, the particle deposition rates are shown in Fig. 8. As can be seen, the particles are collected on the fiber at almost the same deposition rate, regardless of the electrostatic interactions between the oncoming particles and deposited particles. From Fig. 7 and Fig. 8, it is concluded that the deposition pattern of particles on a fiber within an external electric field is greatly influenced by the deposited particles on the fiber, even though the particle deposition rate is constant, irrespective of the electrostatic forces due to particle deposits. In general, the filtration performance of a fibrous filter, such as pressure drop or dust holding capacity, is highly dependent on the structure of the particle deposits. Therefore, the electrostatic forces due to the already deposited particles must be included in the calculation of the particle trajectories.

## 3. Effect of Electrical Conductivity of Particles and Filter Fibers

So far, the particles and fibers have been considered as perfect conductors, whose dielectric constants are infinity. This assumption was based on the comments of other researchers. Kraemer and Johnstone [1955] reported that the resistivities usually encountered in insulators are not large enough to prevent the entire surface of the particles from becoming an equipotential surface in an extremely short time; thus the particle should behave as a conductor. Kirsch [1972] also mentioned in his study using a model filter consisting of capron fibers that in view of the presence of easily ionized impurities and contamination on the fiber surface the dielectric constant of the fiber can be assumed as infinity. Most of the previous

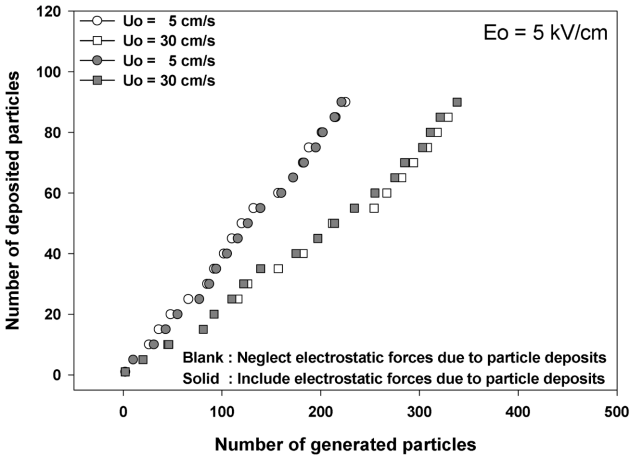


(a) $E_0$ = 5 kV/cm

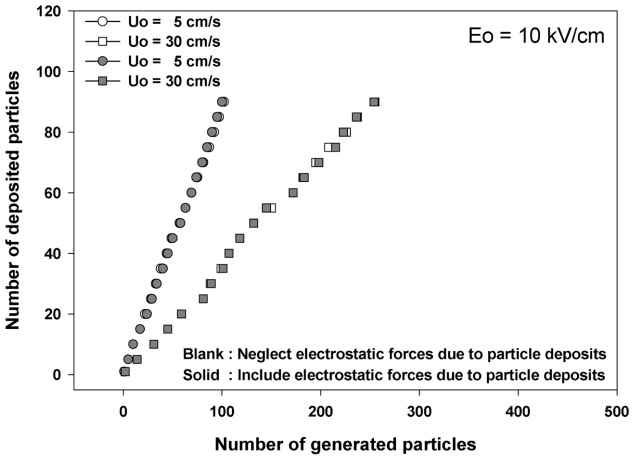


(b) $E_0$ = 10 kV/cm

**Fig. 8. Deposition rate of particles as a result of simulation calculated with and without the electrostatic forces between an approaching particle and the already deposited particles on a fiber at external electric fields of 5 kV/cm and 10 kV/cm.**

theoretical studies on electrically enhanced air filtration, however, have treated dielectric filters and particles as pure dielectrics with their own constants. From those approaches, the real filtration phenomena such as dust loading characteristics can'not be fully understood.

In this section, the effects of the dielectric constants of particles and filter fibers on the structures of particle deposits are analyzed. Especially, the linear structure of the particle dendrites was observed in the experimental studies of Oak and Saville [1980], with an external electric field applied across an isolated fiber.

Fig. 9 compares the particle deposition patterns for conductive fibers and particles with those for dielectrics. The dielectric constants of particles and fibers were assumed to be equal, and set to infinity and 4 for the conductors and dielectrics, respectively. The other variables were fixed as $U_0$=5 cm/s, $E_0$=15 kV/cm, and $\rho_p$=1 g/cm$^3$. In the case of the conductors, the particles tended to build up linear dendrites leading to porous structures. On the other hand, the dielectric particles were deposited in a somewhat irregular pattern, forming less porous deposits. Furthermore, all the conductive particles released

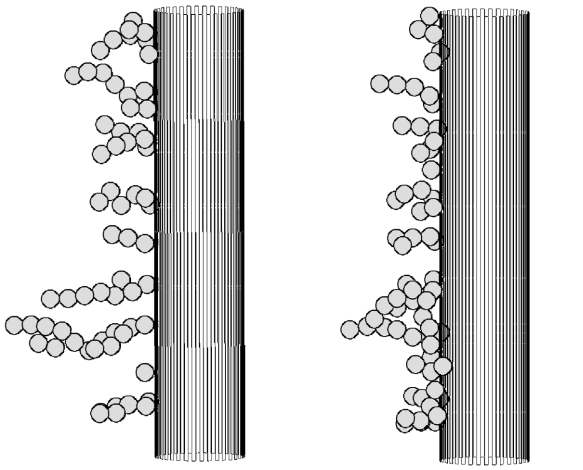

(a) conductive, $\varepsilon_f=\varepsilon_p=\infty$ (b) dielectric, $\varepsilon_f=\varepsilon_p=\infty$

**Fig. 9. Comparison of particle deposition patterns between the conductive and dielectric particles and fibers at $E_0$=15 kV/cm, $U_0$=5 cm/s. $\varepsilon_f$ and $\varepsilon_p$ are the dielectric constants of fiber and particle, respectively.**

from the particle generation plane were perfectly collected on the conductive fiber, while only 64 of the 90 dielectric particles were captured. As expressed in Eqs. (15b) and (16), the dielectric constants are very important factors affecting the magnitude of the polarization forces. For $\varepsilon_f=\varepsilon_p=4$, the magnitude of the parameters is reduced to a fourth of that for conductors. Subsequently, the effect of the dielectrophoretic forces becomes weaker, and the magnitude of the electric forces focused on the tip of particle deposits decreases to an insufficient degree for the formation of a linear dendrite. In Fig. 10, the deposition rates of the particles between the dielectrics and the conductors are compared for external electric fields of 5 and 15 kV/cm, and flow velocities of 5 and 30 cm/s. The deposition rate of the conductive particles was much higher than that of the dielectrics, as the electric force acting on a conductive particle was four times that on a dielectric particle. Especially, the difference in the deposition rates between the dielectrics and conductors is greatly dependent on the dominancy of the electrostatic forces. As mentioned before, the effect of electrostatic forces increases at low flow velocity. Thus, the difference showed a maximum at $E_0$= 5 kV/cm and $U_0$=5 cm/s, and was rapidly reduced at $E_0$=15 kV/cm and $U_0$=5 cm/s. When the electric field is relatively small, the magnitude of the dielectric constants plays a significant role in particle deposition. Conversely, when $E_0$=15 kV/cm and $U_0$=5 cm/s, on the other hand, the effect of the electric field strength was much greater than that of the electrical conductivity; thus the gap in the deposition rate between the dielectrics and the conductors was narrowed. Back to Fig. 9, under the above conditions, although the deposition rates of the conductors and dielectrics had a small discrepancy, the structures of deposits were quite different between them. As a result, it can be concluded that the conductivity of the particles and filter fibers still has big effects on the performance of filters, independently from the electric field strength, at least under the filtration conditions employed in this study.

## 4. Effect of Particle Inertia

Without electrostatic forces, the particles are captured on the filter

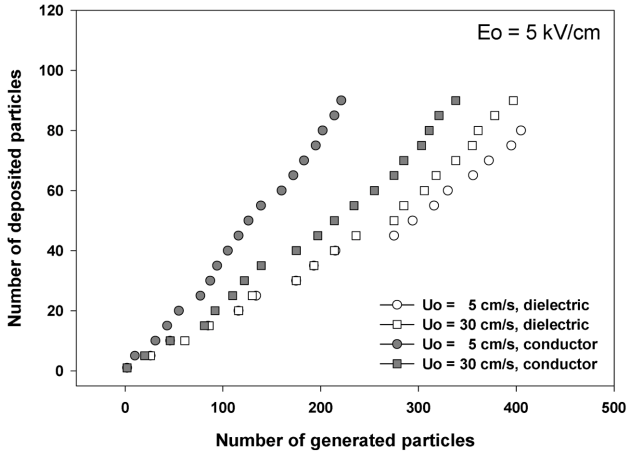


(a) $E_0$ = 5 kV/cm

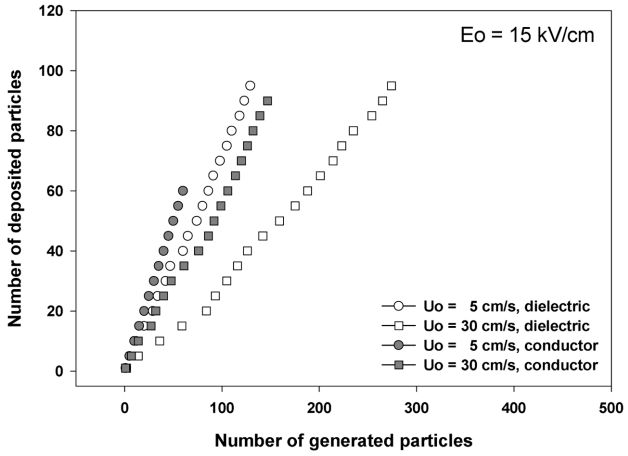


(b) $E_0$ = 15 kV/cm

**Fig. 10. Comparison of deposition rates between the dielectric and conductive fibers and particles at external electric fields of 5 kV/cm and 15 kV/cm, and flow velocities of 5 cm/s and 30 cm/s.**

fibers by diffusion, interception, and inertial impact. In general, the effect of particle inertia on the motion of a particle is represented by a dimensionless parameter called the Stokes number (Stk). In this study, the value of Stk is less than unity. Therefore, it can be expected that the effect of particle inertia might be very small, which has been widely used as an estimation in numerous theoretical studies on air filtration. Many scientists have tried to simplify the equation of particle motion by supposing inertialess particles, and have solved it analytically or numerically. The above assumption has been considered reasonable because the theoretical results were in good agreement with the experimental data.

In this study, the effect of particle inertia on the filtration characteristics was investigated. The deposition rates for various filtration conditions are plotted in Fig. 11. Here, the values of Stk for particles of $\rho_p$=1 g/cm$^3$ are 0.132 and 0.792 at $U_0$=5 and 30 cm/s, respectively. In the absence of electric fields, the particles were deposited at an approximately constant rate in all cases. This means that particle inertia contributes little to the particle deposition. This result supports the assumption of inertialess particles, as mentioned above.

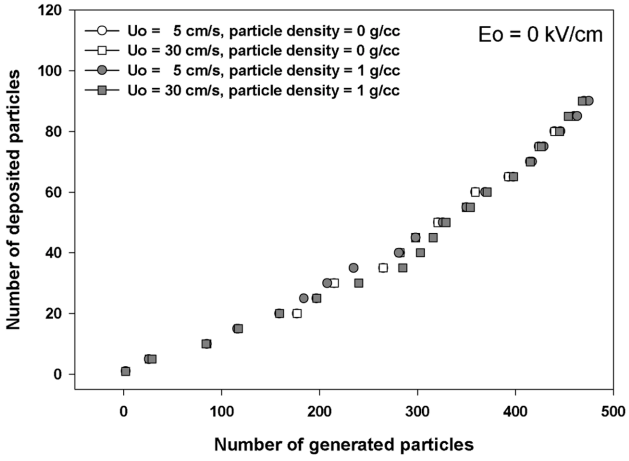


(a) $E_0$ = 0 kV/cm

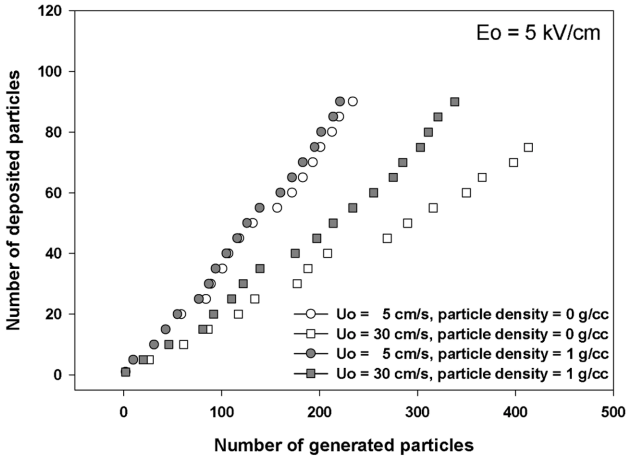


(b) $E_0$ = 5 kV/cm

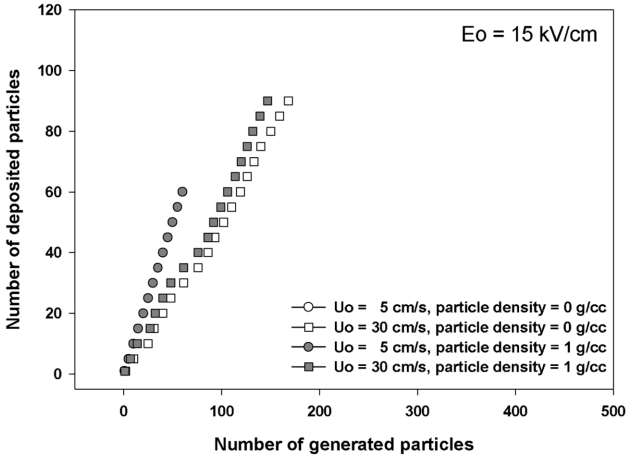


(c) $E_0$ = 15 kV/cm

**Fig. 11. Effect of particle inertia on the particle deposition rate at external electric fields of 0 kV/cm, 5 kV/cm, and 15 kV/cm, and flow velocities of 5 cm/s and 30 cm/s.**

In the case where the electric field of 5 kV/cm was applied, the graph shows different features from those when $E_0$=0 kV/cm. At $U_0$=30 cm/s, the deposition rate of the particles of $\rho_p$=1 g/cm$^3$ was higher than that when they were to be inertialess. This means that

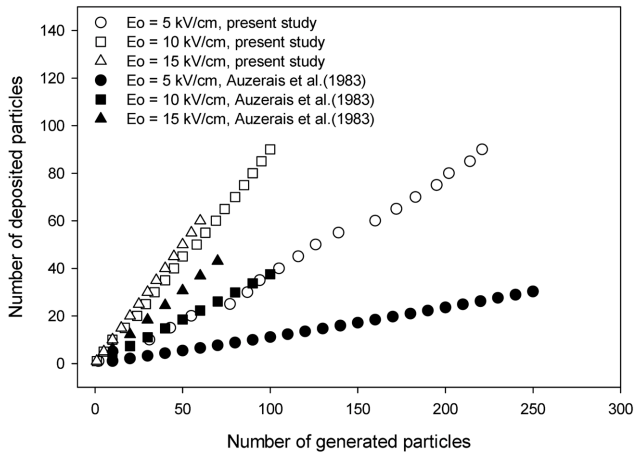


**Fig. 12. Comparison of deposition rates in this study with those of Auzerais et al. [1983] for various electric field strengths at $U_0$=5 cm/s.**

under a specific filtration condition, even the particles of $\rho_p$=1 g/cm$^3$ can have a great effect on the particle deposition. The difference in the deposition rates between inertia and inertialess particles becomes very small at $E_0$=15 kV/cm, as seen in Fig. 11(c), where the electrostatic forces are much more dominant than particle inertia. As a result, it can be stated that the assumption neglecting the particle inertia can introduce an error when predicting the filtration performance, especially in theoretical studies on the particle loading characteristics of electrically enhanced air filters.

## 5. Comparison with Existing Studies

In the present study, the effect of the external electric fields on particle deposition on a fiber was investigated by using a numerical simulation. Auzerais et al. [1983] conducted a similar simulation study to ours. Their study was confined to the low velocity cases so that the particle inertia could be neglected, and the dielectric constants of the particles and fibers were fixed as 4. Fig. 12 shows the deposition rates of the particles for this study and those of Auzerais et al. [1983]. Auzerais et al. [1983] assumed inertialess particles and $\varepsilon_p=\varepsilon_f=4$, while in the present study the particle density was 1 g/cm$^3$ and $\varepsilon_p=\varepsilon_f=\infty$. Flow velocity in both studies was 5 cm/s, and the other conditions were the same as those described in Table 1. In all cases of $E_0$, the deposition rates in this study were much greater than those of Auzerais et al. [1983]. This might be largely attributed to the difference in the conductivity of the particles and fibers between the two studies. As previously mentioned in Fig. 10, the effect of the electrical conductivity was remarkable at low flow velocities.

Another reason for the difference is likely to come from the calculation method for the electrostatic forces between a new particle and already captured particles. Auzerais et al. [1983] treated a dendrite as an ellipsoid, with equal volume and height, and calculated the electrostatic forces between the oncoming particle and the ellipsoid. On the other hand, in the present study, the forces between the newly generated particle and each of captured particles were computed individually. The latter method is more tedious and time-consuming, but more accurate than the former.

This study provides a qualitative insight to the particle deposition characteristics of fibrous filters, using a numerical simulation method,

with an applied homogeneous external electric field. The simulation results are in very good agreement with the existing experimental data, such as Kraemer and Johnstone [1955], Havlicek [1961], Kirsch [1972], Iinoya and Makino [1974], Nelson et al. [1978], Oak and Saville [1980], Wang and Ho [1980], and Oak et al. [1985] in terms of the qualitative aspects. Especially, the linear dendritic structure of the particle deposits, as photographed by Oak and Saville [1980], was exactly simulated in this work.

## CONCLUSIONS

This paper addressed the particle deposition characteristics of fibrous air filters enhanced by an external electric field. Using a Lagrangian simulation method, the trajectories of particles were calculated, and the deposition structures obtained. The effects of the electric field strength, electrostatic forces due to the captured particles, the electrical conductivity of the particles and fibers, and particle inertia on the morphology of the deposits and the deposition rate of particles were investigated.

As the electric field intensity increased, the collection efficiency became higher, and particles were deposited in a linear dendritic form. The linear structure of the particle deposits resulted in the focusing of electrostatic force lines on the tip of particle dendrites. The electrostatic forces due to the deposited particles had a great influence on the particle deposition pattern, although the effect of the forces on the deposition rate was very small. Therefore, the electrostatic interaction between the approaching particles and those previously captured must be taken into account in theoretical studies on the dust loading of electrically enhanced air filters. The morphology of the simulated particle deposits was in good agreement with the others' experimental results.

The electrical conductivity of the particles and filter fibers had a considerable effect on the particle deposition. The conductive particles built up linear dendrites leading to porous structures, while the dielectric particles were deposited in a more irregular and dense form. The deposition rate of the conductive particles was much higher than that of the dielectrics. From this study it was also found that the particle inertia, which has been assumed to be negligible in numerous previous studies on air filtration, could influence the collection efficiency of air filters, with an applied uniform electric field. The particles of only 1 g/cm$^3$ were collected with a higher efficiency than the inertialess particles under specific filtration conditions.

The results of this study agreed very well with those of the previous experimental studies in terms of the qualitative aspects. Specifically, compared with the study of Auzerais et al. [1983], this work predicted much higher collection efficiencies. This was mainly due to the difference in the electrical conductivity of the particles and the filter fibers between the two studies. In the present study, the particles and filter fibers were regarded as perfect conductors, which have been considered to reflect the real filtration phenomena more accurately. Finally, this study is expected to be helpful in understanding filtration properties of electrically enhanced air filters, especially the dust loading of air filters within an external electric field.

## ACKNOWLEDGMENT

This research was performed with the financial support of the Center for Nanostructured Materials Technology under the 21st Century Frontier R&D Program of the Ministry of Science and Technology, Korea.

## NOMENCLATURE

- $A$ : constant, see Eq. (10b)
- $b$ : radius of Kuwabara cell
- $B$ : constant, see Eq. (10b)
- $c$ : packing density of a filter
- $C$ : constant, see Eq. (10b)
- $C_c$ : Cunningham correction factor
- $D$ : constant, see Eq. (10b)
- $d_p$ : particle diameter
- $e$ : elementary charge
- $E$ : electric field strength
- $\vec{E}$ : electric field
- $E_0$ : uniform electric field strength
- $\vec{E}_k$ : electric field around the k-th deposited particle
- $E_r$ : radial component of electric field
- $E_\theta$ : tangential component of electric field
- $E_z$ : z-directional component of electric field
- $E_{r'}$ : radial component of electric field in spherical coordinate system shown in Fig. 1
- $E_{\phi'}$ : longitudinal component of electric field in spherical coordinate system shown in Fig. 1
- $E_{\theta'}$ : latitudinal component of electric field in spherical coordinate system shown in Fig. 1
- $f(n)$ : fraction of particles having n units of charge of one sign, see Eq. (19)
- $\vec{F}_D$ : drag force
- $\vec{F}_E$ : electrostatic force
- $\vec{F}_G$ : gravitational force
- $F^*_{C,r}$ : radial component of dimensionless Columbic force between the approaching particle and fiber
- $F^*_{C,\theta}$ : tangential component of dimensionless Columbic force between the approaching particle and fiber
- $F^*_{C,r'_k}$ : radial component of dimensionless Columbic force between the approaching particle and k-th deposited particle
- $F^*_{C,\theta'_k}$ : latitudinal component of dimensionless Columbic force between the approaching particle and k-th deposited particle
- $F^*_{P,r}$ : radial component of dimensionless dielectrophoretic force between the approaching particle and fiber
- $F^*_{P,\theta}$ : tangential component of dimensionless dielectrophoretic force between the approaching particle and fiber
- $F^*_{P,r_k}$ : radial component of dimensionless dielectrophoretic force between the approaching particle and k-th deposited particle
- $F^*_{P,\theta_k}$ : latitudinal component of dimensionless dielectrophoretic force between the approaching particle and k-th deposited particle
- $\vec{g}$ : gravitational acceleration
- $J$ : constant, see Eq. (10a)
- $k$ : Boltzmann constant
- $Kn$ : Knudsen number
- $m$ : mass of particle
- $n$ : number of elementary charge
- $N$ : total number of deposited particles

$N_C$ : dimensionless parameter, see Eq. (15a)
$N_{P,I}$ : dimensionless parameter, see Eq. (15b)
$N_{P,II}$ : dimensionless parameter, see Eq. (15b)
$N_{REP}$ : dimensionless parameter, see Eq. (15c)
$N_G$ : dimensionless parameter, see Eq. (15c)
$q_p$ : particle charge
$r^*$ : dimensionless radial coordinate in the cylindrical coordinate system
$r'^*_k$ : dimensionless radial coordinate in the spherical coordinate system whose origin is located at the center of the k-th deposited particle
$r_f$ : fiber radius
$r_p$ : particle radius
Re : Reynolds number
Stk : Stokes number, see Eq. (15a)
t : time
T : absolute temperature
$\vec{u}$ : fluid velocity
$U_0$ : magnitude of undisturbed flow velocity
$\vec{v}$ : particle velocity
$(u_x, u_y, u_z)$ : x, y, z components of fluid velocity
$(u^*_x, u^*_y, u^*_z)$ : dimensionless x, y, z components of fluid velocity
$(v_x, v_y, v_z)$ : x, y, z components of particle velocity
$(v^*_x, v^*_y, v^*_z)$ : dimensionless x, y, z components of particle velocity
(x, y, z) : rectangular coordinates
$(x^*, y^*, z^*)$ : dimensionless rectangular coordinates
$(x_0, y_0, z_0)$ : initial position of a particle
(r, q, z) : cylindrical coordinates in Fig. 1
$(r', \phi', \theta')$ : spherical coordinates in Fig. 1
$(r'_k, \phi'_k, \theta'_k)$ : spherical coordinates whose origin is located at the center of the k-th deposited particle as illustrated in Fig. 2

**Greek Letters**

$\alpha$ : constant, see Eq. (16)
$\beta$ : constant, see Eq. (16)
$\varepsilon_f$ : dielectric constant of fiber
$\varepsilon_p$ : dielectric constant of particle
$\lambda$ : mean free path of air molecules
$\mu$ : kinetic viscosity of air
$\rho_{air}$ : air density
$\rho_p$ : particle density

## REFERENCES


Auzerais, F., Payatakes, A. C. and Okuyama, K., "Dendritic Deposition of Uncharged Aerosol Particles on an Uncharged Fiber in the Presence of an Electrical Field," *Chemical Engineering Science*, **38**(3), 447 (1983).

Bai, H., Lu, C. and Chang, C. L., "A Model to Predict the System Performance of an Electrostatic Precipitator for Collecting Polydisperse Particles," *J. of the Air & Waste Management Assoc.*, **45**, 908 (1995).

Barot, D. T., Tien, C. and Wang, C., "Accumulation of Solid Particles on Single Fibers Exposed to Aerosol Flows," *AIChE J.*, **26**(2), 289 (1980).

Baumgartner, H. and Löffler, F., "Three-Dimensional Numerical Simulation of the Deposition of Polydisperse Aerosol Particles on Filter Fibres Extended Concept and Preliminary Results," *J. Aerosol Science*, **18**(6), 885 (1987).

Havlíček, V., "The Improvement of Efficiency of Fibrous Dielectric Filters by Application of an External Electric Field," *Int. J. Air and Water Poll.*, **4**, 225 (1961).

Henry, F. and Ariman, T., "Cell Model of Aerosol Collection by Fibrous Filters in an Electrostatic Field," *J. Aerosol Science*, **12**(2), 91 (1981).

Hinds, W. C. and Kadrichu, N. P., "The Effect of Dust Loading on Penetration and Resistance of Glass Fiber Filters," *Aerosol Science and Technology*, **27**, 162 (1997).

Iinoya, K. and Makino, K., "Application of Electric Field Effects to Dust Collection Filters," *Aerosol Science*, **5**, 357 (1974).

Jennings, S. G., "The Mean Free Path in Air," *J. Aerosol Science*, **19**(2), 159 (1988).

Kanaoka, C. and Hiragi, S., "Pressure Drop of Air Filter with Dust Load," *J. Aerosol Science*, **21**(1), 127 (1990).

Kanaoka, C., Emi, H., Hiragi, S. and Myojo, J., *Morphology of Particulate Agglomerates on a Cylindrical Fiber and a Collection Efficiency of a Dust Loaded Fiber*, 2nd Int. Aerosol Conf., 674 (1986).

Kao, J., Tardos, G. I. and Pfeffer, R., "Dust Deposition in Electrostatically Enhanced Fibrous Filters," *IEEE Transactions on Industry Applications*, **IA-23**(3), 464 (1987).

Keefe, D., Nolan, P. J. and Rich, T. A., "Charge Equilibrium in Aerosols According to the Boltzmann Law," *Proceedings of the Royal Irish Academy*, **60**, 27 (1959).

Kraemer, H. F. and Johnstone, H. F., "Collection of Aerosol Particles in Presence of Electrostatic Fields," *Industrial and Engineering Chemistry*, **47**(12), 2426 (1955).

Kuwabara, S., "The Forces Experienced by Randomly Distributed Parallel Circular Cylinders or Spheres in a Viscous Flow at Small Reynolds Numbers," *J. of the Physical Society of Japan*, **14**(4), 527 (1959).

Nelson, G. O., Bergman, W., Miller, H. H. and Taylor, R. D., "Enhancement of Air Filtration Using Electric Fields," *Am. Ind. Hyg. Assoc. J.*, **39**, 472 (1978).

Nielsen, K. A. and Hill, J. C., "Particle Chain Formation in Aerosol Filtration with Electrical Forces," *AIChE J.*, **26**(4), 678 (1980).

Oak, M. J. and Saville, D. A., "The Buildup of Dendrite Structures on Fibers in the Presence of Strong Electrostatic Fields," *J. of Colloid and Interface Science*, **76**(1), 259 (1980).

Park, H.-S. and Park, Y. O., "Filtration Properties of Electrospun Ultrafine Fiber Webs," *Korean J. Chem. Eng.*, **22**(1), 165 (2005).

Park, Y. O., Park H.-S., Park, S. J., Kim, S. D., Choi, H. K. and Lim, J. H., "Development and Evaluation of Multilayer Air Filter Media," *Korean J. Chem. Eng.*, **18**(6), 1020 (2001).

Payatakes, A. C., "Model of Aerosol Particle Deposition in Fibrous Media with Dendrite-Like Pattern. Application to Pure Interception during Period of Unhindered Growth," *Filtration & Separation*, 602 (1976).

Sakano, T., Otani, Y., Namiki, N. and Emi, H., "Particle Collection of Medium Performance Air Filters Consisting of Binary Fibers under Dust Loaded Conditions," *Separation and Purification Technology*, **19**, 145 (2000).

Shapiro, M., Laufer, G. and Gutfinger, C., "Electric forces in Aerosol Filtration in Fibrous and Granular Filters A Parametric Study," *Atmospheric Environment*, **17**(3), 477 (1983).

Tien, C., Wang, C. and Barot, D. T., "Chainlike Formation of Particle Deposits in Fluid-Particle Separation," *Science*, **196**, 983 (1977).

Walsh, D. C. and Stenhouse, J. I. T., "Parameters Affecting the Loading Behavior and Degradation of Electrically Active Filter Materials," *Aerosol Science and Technology*, **29**, 419 (1998).

Wang, C., "Electrostatic Forces in Fibrous Filters a Review," *Powder Technology*," **118**, 166 (2001).

Wang, C. S., Ho, C. P., Makino, H. and Iinoya, K., "Effect of Electrostatic Fields on Accumulation of Solid Particles on Single Cylinders," *AIChE J*., **26**(4), 680 (1980).

Wu, Z., Walters, J. K. and Thomas, D. W. P., "The Deposition of Particles from an Air Flow on a Single Cylindrical Fiber in a Uniform Electrical Field," *Aerosol Science and Technology*, **30**, 62 (1999).

Zebel, G., "Deposition of Aerosol Flowing Past a Cylindrical Fiber in a Uniform Electric Field," *J. of Colloid Science*, **20**, 522 (1965).